A Controllable Ternary Interpolatory Subdivision Scheme

Hongchan Zheng*, Zhenglin Ye, Zuoping Chen and Hongxing Zhao[1]

Department of Applied Mathematics, Northwestern Polytechnical University, Xi'an 710072, P.R. China
[1] Yulin College Shaanxi, Yulin 719000, P.R. China

Abstract − A non-uniform 3-point ternary interpolatory subdivision scheme with variable subdivision weights is introduced. Its support is computed. The C^0 and C^1 convergence analysis are presented. To elevate its controllability, a modified edition is proposed. For every initial control point on the initial control polygon a shape weight is introduced. These weights can be used to control the shape of the corresponding subdivision curve easily and purposefully. The role of the initial shape weight is analyzed theoretically. The application of the presented schemes in designing smooth interpolatory curves and surfaces is discussed. In contrast to most conventional interpolatory subdivision scheme, the presented subdivision schemes have better locality. They can be used to generate C^0 or C^1 interpolatory subdivision curves or surfaces and control their shapes wholly or locally.

Keywords: Ternary subdivision, Interpolation, C^k-continuity, Shape controllability, Surface modeling

1. Introduction

In recent years subdivision schemes have been important because they provide an efficient way to describes curves, surfaces and other geometric objects. Subdivision schemes can be classified in approximating and interpolating schemes. Interpolation by using subdivision is an attractive feature in more than one way. First, the original control points defining the curve or surface are also points of the limit curve or surface, which allows one to control it in a more intuitive manner. Second, many algorithms can be considerably simplified, and many calculations can be performed "in place".

Most work in the area of interpolatory subdivision curve schemes has considered binary schemes with an even number of control points. Dyn, Levin and Gregory [7] described a 4-point binary interpolatory subdivision scheme (see Fig. 1(a)), which they proved to be C^1-continuous. Cai [1, 2, 3] made this scheme applicable to the case of nonuniform control points, non-uniform subdivision and upgraded the scheme to the modified 4-point scheme which can interpolate the endpoints. Jin [11] and Kuijt [13] presented a nonlinear and a nonuniform 4-point binary interpolatory subdivision scheme respectively. Weissman [16] described a 6-point binary interpolatory subdivision scheme. Deslauriers and Dubuc [4] analyzed 2N-point subdivision schemes derived from polynomial interpolation.

While Hassan mainly focused on the ternary subdivision scheme which generates *three* new control points corresponding to each control point of previous subdivision level by subdivision rules. In [10] he introduced a 4-point ternary interpolating scheme, and in [8] he investigated ternary schemes with three control points. He proposed a 3-point ternary interpolating scheme (see Fig. 1(b)), whose mask was given by

$$\alpha = (\alpha_j) = [..,0,0,a,0,b,1-a-b,1,1-a-b,b,0,a,0,0,...],$$

where a and b are two parameters. Since the subdivision scheme is uniform and stationary, the generating function formalism can be used to analyze its continuity properties. It is proved that when the two parameters a and b are kept within a proper range, it is C^1-continuous. Furthermore for $a = -\frac{1}{15}$, $b = \frac{4}{15}$, its Hölder exponent [9] is $C^{1.46}$. Because of the ternary property of the 3-point ternary interpolating subdivision scheme, we can have a quicker generation of C^1 subdivision curve by using it than by using 4-point binary one.

But from [8] we do not know the intuitionistic meanings of the two parameters a and b and how the parameters affect the shape of the subdivision curve, which limits the application of the subdivision scheme in a way.

The most famous binary interpolatory subdivision surface scheme is the butterfly scheme for triangular meshes proposed in [6]. This scheme is a generalization of the 4-point binary curve subdivision scheme, and was subsequently improved in [17]. Kobbelt [12] described a C^1 binary interpolatory scheme for quadrilateral meshes with arbitrary topology. Labisk [14] introduced an interpolatory $\sqrt{3}$-subdivision scheme. Dodgson [5] considered the construction of a ternary interpolating

*Corresponding author:
Tel: +86-(29) 8849 4181
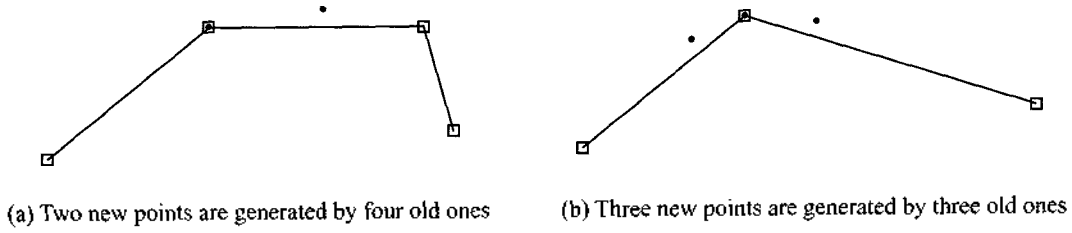Fax: +86-(29)6881 5995
E-mail: zhenghongchan@ry165.com

(a) Two new points are generated by four old ones

(b) Three new points are generated by three old ones

Fig. 1. Generation of new points in the process of the 4-point binary (a) and the 3-point ternary interpolatory subdivision (b), where new points are marked by solid dots, and the old ones are marked by hollow squares.

scheme for the triangular mesh, but the continuity of the limit surface is not known.

With the observation that smooth interpolatory subdivision algorithm, which has good controllability is needed in many practical problems, in this paper, we focus on the construction of a C^1 ternary interpolatory subdivision scheme with good controllability.

Based on the scheme in [8] we first propose a non-uniform and non-stationary 3-point ternary interpolatory subdivision curve scheme with variable subdivision weights which have distinct geometric meaning. The sufficient conditions of the uniform convergence and C^1-continuity of the subdivision scheme are analyzed and proved. To improve the controllability of the subdivision scheme, we introduce a modified non-uniform 3-point ternary interpolatory subdivision scheme. For every initial control point on the initial control polygon a shape weight is introduced. When the subdivision is going on, we refine the control polygon and the weights simultaneously and recursively. The initial shape weights can be used to control the shape of the subdivision curve. The role of initial weight is analyzed theoretically and is demonstrated by a few examples. Then the application of the non-uniform 3-point ternary interpolatory subdivision schemes to the design of smooth curve and surface is discussed. Using our new schemes one can model C^0 or C^1 interpolatory subdivision curves and surfaces and control their shapes wholly or locally.

2. Non-uniform 3-point Ternary Subdivision Scheme

Given the set of initial control points $P^0 = \{P_j^0 \in R^d\}_{j=-1}^{n+1}$, let $P^k = \{P_j^k\}_{j=-1}^{3^k n+1}$ be the set of control points at level k ($k \geq 0$, $k \in Z$), define $\{P_j^{k+1}\}_{j=-1}^{3^{k+1}n+1}$ recursively by the following subdivision rule:

$$\begin{cases} P_{3j-1}^{k+1} = w_j^k P_{j-1}^k + \left(\frac{4}{3}-2w_j^k\right)P_j^k + \left(w_j^k-\frac{1}{3}\right)P_{j+1}^k, & 0 \leq j \leq 3^k n, \\[2mm] P_{3j}^{k+1} = P_j^k, & 0 \leq j \leq 3^k n, \\[2mm] P_{3j+1}^{k+1} = \left(w_j^k-\frac{1}{3}\right)P_{j-1}^k + \left(\frac{4}{3}-2w_j^k\right)P_j^k + w_j^k P_{j+1}^k, & 0 \leq j \leq 3^k n, \end{cases}$$
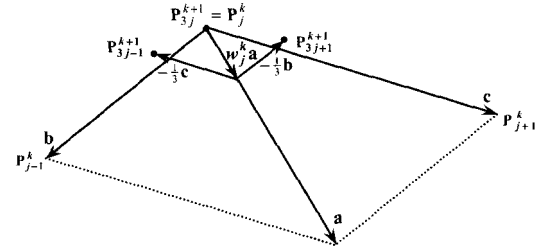
(1)

Fig. 2. Geometric interpretation of the subdivision weight w_j^k.

where w_j^k is a variable subdivision weight with distinct geometric meaning (see Fig. 2). In Fig. 2 new points are marked by black solid dots, where $a = P_{j-1}^k + P_{j+1}^k -2P_j^k$, $b = P_{j-1}^k - P_j^k$, $c = P_{j+1}^k - P_j^k$. Theoretically all the subdivision weights w_j^ks can be chosen arbitrarily, so this scheme is non-uniform and non-stationary.

3. Support of the Non-uniform 3-point Ternary Subdivision Scheme

In this section we calculate the support for the above subdivision scheme before we do the convergence analysis that follows. We consider the limit of the above subdivision scheme with initial control points set

$$\{P_j^0 \in R^2 | P_0^0 = (0, 1), P_j^0 = (j, 0), j = \pm 1, \pm 2, \pm 3, ...\},$$

where the point P_0^0 at 0 is the only control point with non-zero y-ordinate. The subdivision curve after four subdivision steps with $w_j^k = \frac{1}{4}, k \geq 0$ are illustrated in Fig. 3, where the initial control points are marked by solid dots.

At the first subdivision step, we see that the control points $P_{\pm4}^1$ at $\pm\frac{4}{3}$ are the furthest control points with non-zero y-ordinate. At the second subdivision step, we see that the control points $P_{\pm16}^2$ at $\pm\frac{4}{3}(1+\frac{1}{3})$ are the furthest control points with non-zero y-ordinate. By

Fig. 3. Result of the 3-point ternary scheme after four subdivision steps with $w_j^k = \frac{1}{4}$.

recursive analysis we know that after k subdivision steps the furthest control points $P_{\pm x_k}^k$ (where $x_k = 3(x_{k-1} + 1) + 1$, $x_0 = 0$) with non-zero y-ordinate will be at $\pm\frac{4}{3}$ $\left(1 + \frac{1}{3} + \frac{1}{3^2} + \cdots \frac{1}{3^{n-1}}\right)$, hence the total support is

$$2 \times \frac{4}{3}\left(1 + \frac{1}{3} + \frac{1}{3^2} + \cdots \frac{1}{3^{n-1}} + \cdots\right) = 2 \times \frac{4}{3}\sum_{i=1}^{\infty}\frac{1}{3^{i-1}} = 2 \times \frac{4}{3} \times \frac{1}{1-\frac{1}{3}} = 4.$$

This support compares favourably with the 4-point binary scheme having a support of 6 and the 4-point ternary scheme having a support of 5. So the subdivision scheme proposed in this paper has a smaller support and has better locality.

4. Convergence Analysis

To study the convergence property of the above subdivision algorithm and the smooth property of the limit curve, a proper parametrization of the subdivision curve should be introduced. Similar to the dyadic parametrization for a binary subdivision algorithm, here we let P_j^k be the values corresponding to $\frac{j}{3^k}$. The analysis of the subdivision scheme can be reduced to the convergence and continuity of each component of the generated curve. Since each component is a scalar function generated by the same subdivision scheme, it is sufficient to analyze control points in R. To get the sufficient conditions for this subdivision scheme to be uniformly convergent and C^1 we first introduce the following lemmas.

Lemma 1. Let

$$g_1(x) = |x| + \left|\frac{1}{3} - x\right|, \quad g_2(x, y) = \left|\frac{1}{3} - x\right| + |1 - x - y| + \left|\frac{1}{3} - y\right|,$$

$$D_0 = \left\{(x, y)\Big|\frac{1}{6} < x < \frac{2}{3}, \frac{1}{6} < y < \frac{2}{3}, x \in R, y \in R\right\},$$

then for $\frac{1}{6} < x < \frac{2}{3}$, $g_1(x) < 1$, and for $(x, y) \in D_0$, $g_2(x,y) < 1$.

Lemma 2. Let

$$g_3(x, y) = |2 - 6x| + |3y - 1|, \quad g_4(y) = |6y - 1|,$$

$$D_1 = \left\{(x, y)\Big|\frac{2}{9} < x < \frac{1}{3}, \frac{2}{9} < y < \frac{1}{3}, x \in R, y \in R\right\},$$

then for $(x, y) \in D_1$, $g_3(x, y) < 1$, $g_3(y, x) < 1$, and for $\frac{2}{9} < y < \frac{1}{3}$, $g_4(y) < 1$.

By computing we can find the two Lemmas are true. Here we will not give the details.

Theorem 1. Given the initial data $\{f_j^0 \in R\}_{j=-1}^{n+1}$, let f_j^{k+1}

be the values corresponding to $\frac{j}{3^{k+1}}$ ($-1 \le j \le 3^{k+1} n + 1$, $k \ge 0$), f_j^{k+1} are defined by

$$\begin{cases} f_{3j-1}^{k+1} = w_j^k f_{j-1}^k + \left(\frac{4}{3} - 2w_j^k\right)f_j^k + \left(w_j^k - \frac{1}{3}\right)f_{j+1}^k, & 0 \le j \le 3^k n, \\ f_{3j}^{k+1} = f_j^k, & 0 \le j \le 3^k n, \\ f_{3j+1}^{k+1} = \left(w_j^k - \frac{1}{3}\right)f_{j-1}^k + \left(\frac{4}{3} - 2w_j^k\right)f_j^k + w_j^k f_{j+1}^k, & 0 \le j \le 3^k n. \end{cases}$$

Then for $\frac{1}{6} < w_j^k < \frac{2}{3}$, $j = -1, 0, \cdots, 3^k n + 1$, $k \ge 0$, there exists a function $f \in C[0, n]$ such that

$$f\left(\frac{j}{3^k}\right) = f_j^k, \quad 0 \le j \le 3^k n, \quad k \ge 0.$$

Proof. Let f^k be the piecewise linear interpolation of $\{f_j^k\}_{j=-1}^{3^k n+1}$. It is clear that the maximal error between the functions f^k and f^{k+1} can be attained at the points

$\left\{\frac{3j+1}{3^{k+1}}\right\}_{j=0}^{3^k n}$ and $\left\{\frac{3j+2}{3^{k+1}}\right\}_{j=-1}^{3^k n-1}$, and its value is

$$f^{k+1}\left(\frac{3j+1}{3^{k+1}}\right) - f^k\left(\frac{3j+1}{3^{k+1}}\right) = f_{3j+1}^{k+1} - \frac{1}{3}(2f_j^k + f_{j+1}^k)$$

$$= \left(\frac{1}{3} - w_j^k\right)(f_j^k - f_{j-1}^k) + \left(w_j^k - \frac{1}{3}\right)(f_{j+1}^k - f_j^k),$$

$$f^{k+1}\left(\frac{3j+2}{3^{k+1}}\right) - f^k\left(\frac{3j+2}{3^{k+1}}\right) = f_{3j+2}^{k+1} - \frac{1}{3}(f_j^k + 2f_{j+1}^k)$$

$$= \left(\frac{1}{3} - w_j^k\right)(f_{j+1}^k - f_j^k) + \left(w_j^k - \frac{1}{3}\right)(f_{j+2}^k - f_{j+1}^k).$$

Let $|\cdot|_\infty$ denote the maximum norm on $[0, n]$. Then for $\frac{1}{6} < w_j^k < \frac{2}{3}$, $j = -1, 0, \cdots, 3^k n + 1$, we get

$$\left|f^{k+1} - f^k\right|_\infty = \max_{0 \le t \le n}\left|f^{k+1}(t) - f^k(t)\right| < \frac{2}{3}\max_{-1 \le j \le 3^k n}\left|f_{j+1}^k - f_j^k\right|.$$
$$\tag{2}$$

By estimating $\left|f_{j+1}^k - f_j^k\right|$, we can obtain

$$\max_{-1 \le j \le 3^k n}\left|f_{j+1}^k - f_j^k\right| \le M_0 \max_{-1 \le j \le 3^{k-1} n}\left|f_{j+1}^{k-1} - f_j^{k-1}\right|, \tag{3}$$

where $M_0 = \max\left\{\left|w_j^{k-1}\right| + \left|\frac{1}{3} - w_j^{k-1}\right|, \left|w_{j+1}^{k-1}\right| + \left|\frac{1}{3} - w_{j+1}^{k-1}\right|,\right.$

$$\left.\left|\frac{1}{3} - w_j^{k-1}\right| + \left|1 - w_j^{k-1} - w_{j+1}^{k-1}\right| + \left|\frac{1}{3} - w_{j+1}^{k-1}\right|\right\}.$$

Let $w_j^{k-1} = x$, $w_{j+1}^{k-1} = y$, based on Lemma 1 we can obtain that for $(x, y) \in D_0$,

$$M_0 = \max_{(x,y) \in D_0}\{g_1(x), g_1(y), g_2(x,y)\} < 1. \tag{4}$$

By (2), (3) and (4), we finally get the sequence of continuous functions $\{f^k\}$ is a Cauchy sequence, so there exists a continuous function $f \in C[0,n]$ such that

$$\lim_{k \to +\infty} f^k = f.$$

This complete the proof since obviously $f^m\left(\dfrac{j}{3^k}\right) = f_j^k$, for all $0 \le j \le 3^k n$ and any $m \ge k$.

Theorem 2. For $\dfrac{2}{9} < w_j^k < \dfrac{1}{3}, j = -1, 0, \ldots, 3^k n + 1, k \ge 0$,

the limit function f in Theorem 1 is C^1 in the interval $[0, n]$.

Proof. Consider the divided differences

$$d_j^k = 3^k(f_{j+1}^k - f_j^k), -1 \le j \le 3^k n,$$

and let d^k be the piecewise linear interpolation of $\{d_j^k\}_{j=-1}^{3^k n}$. It is easy to note that the maximal error between the functions d^k and d^{k+1} is attained at the points $\left\{\dfrac{j}{3^{k+1}}\right\}_{j=-1}^{3^{k+1}n}$. Similar to the proof of Theorem 1, we can get for $\dfrac{2}{9} < w_j^k < \dfrac{1}{3}, j = -1, 0, \ldots, 3^k n + 1$,

$$|d^{k+1} - d^k|_\infty = \max_{0 \le t \le n} |d^{k+1}(t) - d^k(t)| \le \max_{-1 \le j \le 3^k n - 1} |d_{j+1}^k - d_j^k|. \quad (5)$$

By estimating $|d_{j+1}^k - d_j^k|$, we can obtain

$$\max_{-1 \le j \le 3^k n - 1} |d_{j+1}^k - d_j^k| \le M_1 \max_{-1 \le j \le 3^{k-1} n - 1} |d_{j+1}^{k-1} - d_j^{k-1}|. \quad (6)$$

where $M_1 = \max \{|2 - 6w_j^{k-1}| + |3w_{j+1}^{k-1} - 1|, |3w_j^{k-1} - 1|$

$+ |2 - 6w_j^{k-1}|, |6w_{j+1}^{k-1} - 1|\}$. Let $w_j^{k-1} = x, w_{j+1}^{k-1} = y$, based on Lemma 2 we can obtain that for $(x,y) \in D_1$,

$$M_1 = \max_{(x,y) \in D_1} \{g_3(x,y), g_3(y,x), g_4(y)\} < 1. \quad (7)$$

By (5), (6) and (7), we finally get the sequence of continuous functions $\{d^k\}$ is a Cauchy sequence, so there exists a continuous function d such that

$$\lim_{k \to +\infty} d^k = d.$$

It remains to show that $d = f'$, where f is the limit function of the process. Consider the Bernstein polynomial for the data $\{f_j^k\}$ on $[0, n]$

$$b_k(x) = \sum_{j=0}^{3^k n} C_{3^k n}^j \left(\dfrac{x}{n}\right)^j \left(1 - \dfrac{x}{n}\right)^{3^k n - j} f_j^k,$$

then its derivative is the Bernstein polynomial for the data $\{d_j^k\}$

$$b'_k(x) = \sum_{j=0}^{3^k n - 1} C_{3^k n - 1}^j \left(\dfrac{x}{n}\right)^j \left(1 - \dfrac{x}{n}\right)^{3^k n - 1 - j} d_j^k.$$

From the uniform convergence of the Bernstein polynomials we can get

$$\lim_{k \to +\infty} b_k = f, \quad \lim_{k \to +\infty} b'_k = d,$$

hence $f \in C^1[0,n]$.

From Theorem 1 and Theorem 2 we can conclude that the non-uniform 3-point ternary interpolatory subdivision scheme proposed in this paper can be C^0 or C^1 when all the weights w_j^k s are kept in a certain range respectively. But it is a little hard to know how to have a direct operation to control the shape of the corresponding subdivision curve by using this scheme, because the weights are somewhat arbitrary and free. To increase its controllability, we propose a modified non-uniform 3-point ternary interpolatory subdivision scheme.

5. Modified Non-uniform 3-point Ternary Subdivision Scheme

In this section we alter the subdivision scheme (1). We introduce a shape weight for every initial control point on the initial control polygon. When the subdivision is going on, we refine the control polygon and the weights simultaneously and recursively. The initial shape weights can be used to control the shape of the subdivision curve.

Given the set of initial weights $w^0 = \{w_j^0\}_{j=-1}^{n+1}$ corresponding to the set of initial control points $P^0 = \{P_j^0 \in R^d\}_{j=-1}^{n+1}$, let $P^k = \{P_j^k\}_{j=-1}^{3^k n + 1}$ be the set of control points at level $k(k \ge 0, k \in Z)$, define $\{P_j^{k+1}\}_{j=-1}^{3^{k+1} n + 1}$ recursively by (1), where the shape weights $w_j^k, j = -1, 0, 1, \ldots, 3^k n + 1$ at level $k(k \ge 1, k \in Z)$ are refined recursively by the following subdivision rule:

$$\begin{cases} w_{3j-1}^k = \mu w_{j-1}^{k-1} + (1 - \mu - v)w_j^{k-1} + v w_{j+1}^{k-1}, 0 \le j \le 3^{k-1} n, \\ w_{3j}^k = w_j^{k-1}, 0 \le j \le 3^{k-1} n, \\ w_{3j+1}^k = v w_{j-1}^{k-1} + (1 - \mu - v)w_j^{k-1} + \mu w_{j+1}^{k-1}, 0 \le j \le 3^{k-1} n. \end{cases}$$

$$(8)$$

Here μ, v are two parameters introduced to improve the local and fine controllability of the shape of the subdivision curve.

Remark: For $w_j^0 = \dfrac{1}{3}$ we have $w_j^k \equiv \dfrac{1}{3}, k \ge 1$. From Theorem 1 we can conclude that the limit curve is C^0, which is exactly the initial control polygon.

Based on Theorem 1 and Theorem 2, we have the following theorem.

Theorem 3. For arbitrary $(\mu, v) \in D = \{(\mu, v) | 0 \le \mu \le 1, 0 \le v \le 1, \mu + v \le 1, \mu \in R, v \in R\}$, if the initial weights satisfy $\dfrac{1}{6} < w_j^0 < \dfrac{2}{3}, j = -1, 0, \ldots, n + 1$, the limit function f will

be C^0 at least in the interval $[0, n]$, and especially, if $\frac{2}{9}<w_j^0<\frac{1}{3}$, $j=-1, 0,\ldots, n+1$, the limit function f will be C^1 in the interval $[0, n]$.

From Theorem 3 we know that we can model C^0 or C^1 interpolatory curves and control their shapes by choosing the initial weights w_j^0 s of the control points and parameters μ, v in a proper range.

To analyze the controllability of the presented scheme, we need to discuss how the shape weights affect the shape of the limit curve.

6. The Role of Shape Weight

In this section we analyze the effect of the shape weight w_j^0 on the shape of subdivision curve near the initial control point P_j^0. For simplicity we only need to analyze that of weight w_0^0 on the shape of subdivision curve near the initial control point P_0^0.

From subdivision rules (1) and (8) we have $w_0^k \equiv w_0^0$,

$$P_0^k \equiv P_0^0,\ k \geq 1,\ \text{and } P_{-1}^{k+1}=w_0^k P_{-1}^k+\left(\frac{4}{3}-2w_0^k\right)P_0^k+\left(w_0^k-\frac{1}{3}\right)P_1^k,$$

$$P_1^{k+1}=\left(w_0^k-\frac{1}{3}\right)P_{-1}^k+\left(\frac{4}{3}-2w_0^k\right)P_0^k+w_0^k P_1^k.$$

Let $U_k=P_1^k-P_{-1}^k,\ V_k=P_1^k-P_0^k,\ W_k=P_0^k-P_{-1}^k,$

then $U_k=V_k+W_k$ and $U_{k+1}=\frac{1}{3}U_k=\cdots=\left(\frac{1}{3}\right)^{k+1}(P_1^0-P_{-1}^0),$

$$V_{k+1}=\left(\frac{1}{3}-w_0^k\right)W_k+w_0^k V_k=\left(\frac{1}{3}-w_0^k\right)(U_k-V_k)+w_0^k V_k$$

$$=\left(\frac{1}{3}-w_0^k\right)U_k+\left(2w_0^k-\frac{1}{3}\right)V_k.$$

So we have the following difference equation:

$$V_{k+1}-\left(2w_0^0-\frac{1}{3}\right)V_k=\left(\frac{1}{3}-w_0^0\right)U_k.$$

Since $V_0=P_1^0-P_0^0$, its special solution is

$$V_k=c_1\left(2w_0^0-\frac{1}{3}\right)^k+c_2\left(\frac{1}{3}\right)^k,\qquad(9)$$

where $c_1=\frac{1}{2}(P_1^0+P_{-1}^0-2P_0^0),\ c_2=\frac{1}{2}(P_1^0-P_{-1}^0).$

Similarly we have difference equation:

$$W_{k+1}-\left(2w_0^0-\frac{1}{3}\right)W_k=\left(\frac{1}{3}-w_0^0\right)U_k.$$

Since $W_0=P_0^0-P_{-1}^0$, its special solution is

$$W_k=-c_1\left(2w_0^0-\frac{1}{3}\right)^k+c_2\left(\frac{1}{3}\right)^k.\qquad(10)$$

Now we can depict the effect of weight $w_0^k \equiv w_0^0$ on

the shape of subdivision curve near the control points $P_0^k \equiv P_0^0$ at any subdivision level k. From (9) and (10), we have

$$P_{-1}^k=P_0^0+c_1\left(2w_0^0-\frac{1}{3}\right)^k-c_2\left(\frac{1}{3}\right)^k.$$

Case 1: $\frac{1}{6}<w_0^0<\frac{1}{3}$. Since $0<2w_0^0-\frac{1}{3}<\frac{1}{3}$, the two points P_1^k, P_{-1}^k are always out of the triangle generated by the three points P_{-1}^0, P_0^0, P_1^0 (see Fig. 4). And if $w_0^0 \in \left(\frac{1}{6},\frac{1}{3}\right)$ is decreasing, the two points P_1^k, P_{-1}^k will deviate from the edges $P_0^0 P_1^0$ and $P_0^0 P_{-1}^0$ respectively and gradually. Thus the local limit curve segment near the point P_0^0 will tend to be flat (see Fig. 7(a), in this figure the subdivision curve tends to be flat around the control point P_3^0 (the middle one) compared with Fig. 7(b)).

On the other side when $w_0^0 \in \left(\frac{1}{6},\frac{1}{3}\right)$ is increasing, the two points P_1^k, P_{-1}^k will approximate the edges $P_0^0 P_1^0$ and $P_0^0 P_{-1}^0$ respectively. Thus the local limit curve segment near the point P_0^0 will locally bend more and more (see Fig. 7(b)).

Case 2: $w_0^0=\frac{1}{3}$. In this case the two points P_1^k, P_{-1}^k are always on the edges $P_0^0 P_1^0$ and $P_0^0 P_{-1}^0$ respectively. Thus the local limit curve segment near the point P_0^0 will be the initial control linear segment itself (see Fig. 8).

Case 3: $\frac{1}{3}<w_0^0<\frac{2}{3}$. Since $2w_0^0-\frac{1}{3}>\frac{1}{3}$, the two points P_1^k, P_{-1}^k are always in the triangle generated by the three points P_{-1}^0, P_0^0, P_1^0 (see Fig. 5). And when $w_0^0 \in \left(\frac{1}{3},\frac{2}{3}\right)$ is increasing, the two points P_1^k, P_{-1}^k will deviate from the edges $P_0^0 P_1^0$ and $P_0^0 P_{-1}^0$ respectively and gradually. Thus the local limit curve segment near the point P_0^0 between the point P_{-1}^0 and P_1^0 will have more
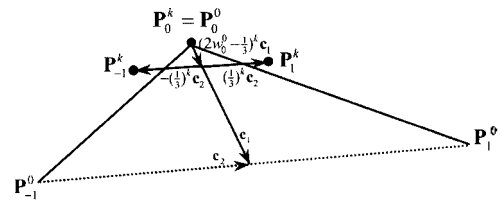
Fig. 4. The case of $\frac{1}{6}<w_0^0<\frac{1}{3}$.
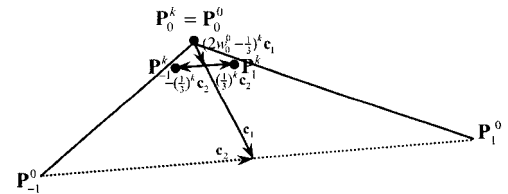
Fig. 5. The case of $\frac{1}{3}<w_0^0<\frac{2}{3}$.

and more inflexions as viewed from the whole curve. In fact in this case the limit curve will be fractal-like curve.

7. Application of the Non-uniform 3-point Scheme to Curve Modeling

The presented subdivision schemes can be used for the design of a C^1 or C^0 interpolatory curve that interpolates a set of control points $\{P_0^0, P_1^0, ..., P_n^0\}$. In the case of open curves, we need to supply two additional control points P_{-1}^0 and P_{n+1}^0, which affect the behavior of the curve near its end points P_0^0 and P_n^0. In the case of a closed curve, we only need to let $P_{-1}^0 = P_n^0$ and $P_{n+1}^0 = P_0^0$.

Furthermore, it can be used to control the shapes of the interpolatory subdivision curves freely. We can control the shapes of curves to a great extent by adjusting the initial control points. In the case of given control points, we can control them by adjusting the weights and the parameters.

We may have an entire control of them by setting $w_j^k \equiv w$ (constant), then we will control them macro-cosmically by choosing the value of w. Fig. 6 shows an example of closed interpolatory curves after four subdivision steps. The set of initial control points is

$$\{(-1,0),\left(0,\frac{1}{2}\right)(1,0),(1,-1),(3,-1),(3,1),\left(0,\frac{5}{2}\right)(-3,1),$$

$$(-3,-1)(-1,-1)\}.$$

In Fig. 6 the control polygon is drawn by a dash-dotted line, the smooth curve obtained by our scheme with $w=\frac{1}{4}$ is marked by a full line and that with $w=\frac{5}{18}$ by a dashed line. From Theorem 3 we know that in both cases the limit curves will be C^1.

The more important thing is that we can have a local control of them easily and efficiently. For example, if we want to control the shapes of the curves near a specified control point P_i^0, we can achieve this by adjusting the corresponding weight w_i^0 and selecting parameters μ, ν.

The following two examples show the curves applied (1) and (8) to the same control polygon after five subdivision steps respectively. The control polygons are drawn by dashed lines, and the subdivision curves
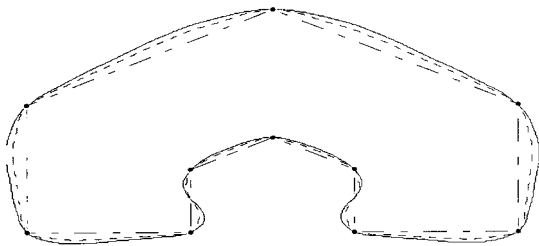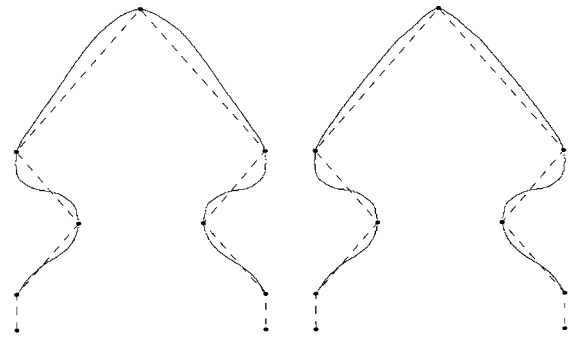

Fig. 6. 3-point ternary interpolatory curve.

(a) $w_3^0 = \frac{1}{4}$ (b) $w_3^0 = \frac{5}{18}$

Fig. 7. The effect of the weight w_3^0 on the subdivision curve segment near the control point P_3^0 (the middle one).

are drawn by full lines.

Fig. 7 shows the results of the adjusting the weight w_3^0 corresponding to the control point is P_3^0 (the middle one) to control the shapes of the open curves locally. The set of initial control points is $\{(-1,-1),$

$\left(-\frac{1}{2},0\right),(-1,1)$ $(0,3),(1,1),\left(\frac{1}{2},0\right),(1,-1)\}$, the two additional control points are $\left(-1,-\frac{3}{2}\right)$ and $\left(1,-\frac{3}{2}\right)$. In Fig. 7(a) we specify the set of initial weights $w^0 = \left\{\frac{1}{4},\frac{1}{4},\frac{1}{4},\frac{1}{4},\frac{1}{4},\frac{1}{4},\right.$

$\left.\frac{1}{4},\frac{1}{4},\frac{1}{4}\right\}$, while in Fig. 7(b) we specify $w^0 = \left\{\frac{1}{4},\frac{1}{4},\frac{1}{4},\frac{1}{4},\right.$

$\left.\frac{5}{18},\frac{1}{4},\frac{1}{4},\frac{1}{4},\frac{1}{4}\right\}$. In both cases we let $\mu = \nu = 0$, so from Theorem 3 we know that both limit curves will be C^1.

Fig. 8 shows the results of the fine control of the shapes of the curves near a control point by selecting parameters μ, ν when the set of initial weights w^0 is given. Fig. 8(a) and (b) show two open curves. The set of initial control points is $\{(-3,4)(-1,4),(-2,5),(0,7),(2,5)(1,4)(3,4)\}$, and the two additional control points are $\left(-4,\frac{7}{2}\right)$ and $\left(4,\frac{7}{2}\right)$. In Fig. 8(a) and Fig. 8(b) we specify $w^0 = \left\{\frac{1}{3},\frac{1}{3},\frac{1}{3},\frac{1}{3},\frac{1}{4},\frac{1}{3},\frac{1}{3},\frac{1}{3},\frac{1}{3}\right\}$, but in Fig. 8(a) we set $\mu = \nu = 0$, while in Fig. 8(b) we set $\mu=\frac{2}{3}, \nu=\frac{1}{4}$. From Theorem 3 we know that in both cases the limit curves will be C^0. Fig. 8(c) and (d) show two closed curves. The set of initial control points is $\left\{\left(-1,-\frac{3}{2}\right),(-1,-1),\left(-\frac{3}{2},0\right),(-1,1),(0,3),(1,1)\right\}$. Here we specify $w^0 = \left\{\frac{1}{4},\frac{1}{4},\frac{1}{4},\frac{1}{4},\frac{1}{3},\frac{1}{4}\right\}$, but in Fig. 8(c) we set $\mu = \nu = 0$, while in Fig. 8(d) we set $\mu=\frac{9}{5}, \nu=0$.

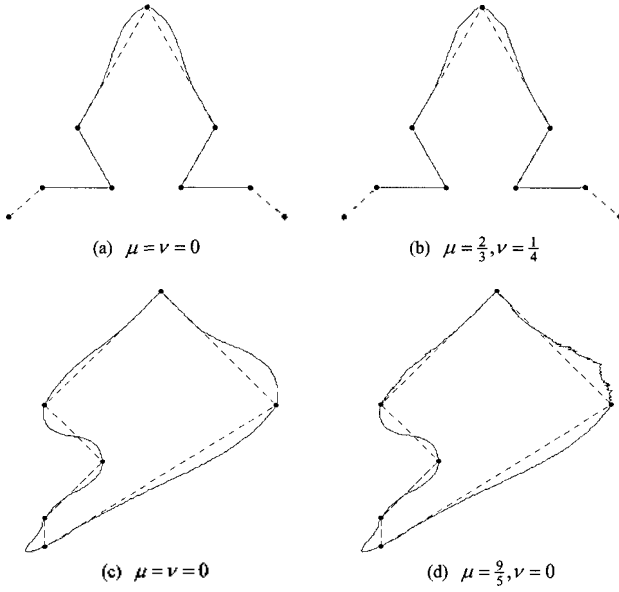Many examples show that when $\mu, \nu \in (0, 1)$ is increasing, their fine effect on the shape of the

(a) $\mu = v = 0$ (b) $\mu = \frac{2}{3}, v = \frac{1}{4}$

(c) $\mu = v = 0$ (d) $\mu = \frac{9}{5}, v = 0$

Fig. 8. The fine effect of the parameters μ, v on the local subdivision curve segment near a control point.

subdivision curve is becoming clear, and when any of them is more than one and increasing, the local limit curve segment will have more and more inflexions.

Hence, given control points, we can control the shape of the interpolatory subdivision curve by adjusting the weights w_i^0 s and the parameters μ, v. The implementation can speed up the generation and the display of a subdivision curve due to the ternary property of the scheme.

8. Application of the Non-uniform 3-point Scheme to Surface Modeling

The presented subdivision schemes can be used to the design of an interpolatory surface.

8.1. Modeling a ternary interpolatory surface based on quadrilateral meshes

We can extend the presented subdivision scheme (1) to the design of a tensor-product 3-point ternary interpolatory subdivision surface based on regular quadrilateral meshes. Here we perform a 1-to-9 quadrilateral split for every quadrilateral face: we leave all the old vertices unchanged, tri-sect all the edges by inserting two new edge-points between every adjacent pair of old ones, and introduce four new face-points corresponding to a face in the old control net.

Given control points

$$\mathbf{P}_{i,j}^0 \in \mathbf{R}^d, i=-1,0,\cdots n+1, j=-1,0,\cdots m+1,$$

at subdivision level $k+1 (k \geq 0, k \in \mathbf{Z})$ first we let

$$\mathbf{P}_{3i,3j}^{k+1} = \mathbf{P}_{i,j}^k, i=,0,\cdots 3^k n, j=0,\cdots 3^k m.$$

Then we apply (1) to index i, introducing two column

edge-points $\mathbf{P}_{3i-1,3j}^{k+1}$, $\mathbf{P}_{3i+1,3j}^{k+1}$ near $\mathbf{P}_{i,j}^k, i=0,1,\cdots,3^k n$,

$j=-1,0,\cdots,3^k m+1$. Finally we apply (1) to the index j and introduce two row edge-points $\mathbf{P}_{i,3j-1}^{k+1}$, $\mathbf{P}_{i,3j+1}^{k+1}$ near

$\mathbf{P}_{i,3j}^{k+1}, i=-1,0,\cdots,3^{k+1}n+1, j=0,\cdots, 3^k m$. The above process can be expressed as the following subdivision rule:

$$
\left\{
\begin{aligned}
&\mathbf{P}_{3i,3j}^{k+1} = \mathbf{P}_{i,j}^k, 0 \leq i \leq 3^k n, 0 \leq i \leq 3^k m,\\
&\mathbf{P}_{3i-1,3j}^{k+1} = w_{i,j}^k \mathbf{P}_{i-1,j}^k + \left(\frac{4}{3}-2w_{i,j}^k\right)\mathbf{P}_{i,j}^k + \left(w_{i,j}^k-\frac{1}{3}\right)\mathbf{P}_{i+1,j}^k,\\
&\qquad 0 \leq i \leq 3^k n, -1 \leq j \leq 3^k m+1,\\
&\mathbf{P}_{3i+1,3j}^{k+1} = \left(w_{i,j}^k-\frac{1}{3}\right)\mathbf{P}_{i-1,j}^k + \left(\frac{4}{3}-2w_{i,j}^k\right)\mathbf{P}_{i,j}^k + w_{i,j}^k \mathbf{P}_{i+1,j}^k,\\
&\qquad 0 \leq i \leq 3^k n, -1 \leq j \leq 3^k m+1,\\
&\mathbf{P}_{i,3j-1}^{k+1} = w_{i,j}^k \mathbf{P}_{i,3j-3}^{k+1} + \left(\frac{4}{3}-2w_{i,j}^k\right)\mathbf{P}_{i,3j}^{k+1} + \left(w_{i,j}^k-\frac{1}{3}\right)\mathbf{P}_{i,3j+3}^{k+1},\\
&\qquad -1 \leq i \leq 3^{k+1}n+1, 0 \leq j \leq 3^k m,\\
&\mathbf{P}_{i,3j+1}^{k+1} = \left(w_{i,j}^k-\frac{1}{3}\right)\mathbf{P}_{i,3j-3}^{k+1} + \left(\frac{4}{3}-2w_{i,j}^k\right)\mathbf{P}_{i,3j}^{k+1} + w_{i,j}^k \mathbf{P}_{i,3j+3}^{k+1},\\
&\qquad -1 \leq i \leq 3^{k+1}n+1, 0 \leq j \leq 3^k m.
\end{aligned}
\right.
$$

After we get all the control points

$$\mathbf{P}_{i,j}^{k+1}, i=-1,0,\ldots 3^k n+1, j=-1,0,\ldots 3^k m+1$$

at step $k+1$, we can generate a refined regular quadrilateral mesh by connecting each control point $\mathbf{P}_{i,j}^{k+1}$ to $\mathbf{P}_{i,j\pm1}^{k+1}$ and $\mathbf{P}_{i\pm1,j}^{k+1} (k \geq 0)$. It is easy to see that we will get a $(3m + 1) \times (3n + 1)$ refinement mesh after one step of tensor-product 3-point ternary interpolatory subdivision to a regular $(m + 1) \times (n + 1)$ quadrilateral mesh.

Letting k tend to infinity, this process will define a C^0 surface from Theorem 1 for $\forall w_{i,j}^k \in \left(\frac{1}{6},\frac{2}{3}\right)$ and a C^1 surface from Theorem 2 for $\forall w_{i,j}^k \in \left(\frac{2}{9},\frac{1}{3}\right)$ due to the property of the tensor-product surface. The limit surface passes through the initial control points $\mathbf{P}_{i,j}^0$, $i = 0 \cdots n$, $j = 0, \cdots m$.

Fig. 9 shows the results of applying the tensor-product 3-point ternary interpolatory subdivision scheme four times. Fig. 9(a) depicts the initial control mesh. Fig. 9(b) shows the result obtained with $w_{i,j}^k = \frac{1}{4}$. Fig. 9(c) describes the result obtained with $w_{i,j}^0 = \frac{5}{18}$ and $w_{i,j}^k = \frac{1}{4}, k > 0$.

From Fig. 9 we know that we can adjust the shape of the subdivision surface by choosing the weights appropriately. Furthermore, because of the ternary and simple property of the tensor-product 3-point inter-
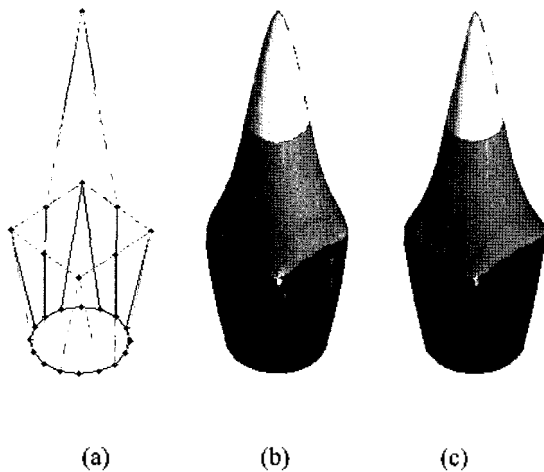
(a)   (b)   (c)

Fig. 9. Examples of tensor-product 3-point ternary interpolatory subdivision.

polatory subdivision scheme the implementation is fast and effective. In practice generally we can get a "good" approximation to the limit surface only after 4~5 subdivision steps. Similarly a modified tensor-product 3-point ternary interpolatory subdivision algorithm including parameters μ, v based on regular quadrilateral mesh can be constructed, which is effective too.

8.2. Modeling a ternary interpolatory surface based on triangular meshes

Similar to the method of Dodgson [5] we can extend the presented subdivision scheme to the design of a ternary interpolatory subdivision surface based on regular triangular meshes. We perform a 1-to-9 triangular split for every triangular face: we leave all the old vertices unchanged, tri-sect all the edges by inserting two new edge-points between every adjacent pair of old ones, and introduce one new face-points corresponding to a face in the old control net. In the case of uniform and stationary subdivision ($w_j^k \equiv w$ (constant)), the subdivision rules are:

(1) New face-point F (see Fig. 10) for a triangle is computed according to the following rule:

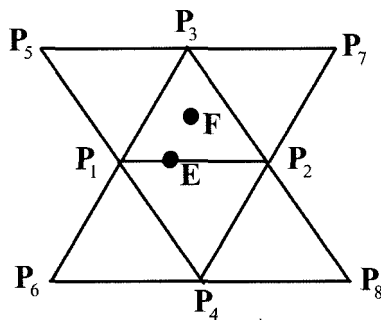$$F = \eta(P_1 + P_2 + P_3) + \kappa(P_4 + P_5 + P_7),$$
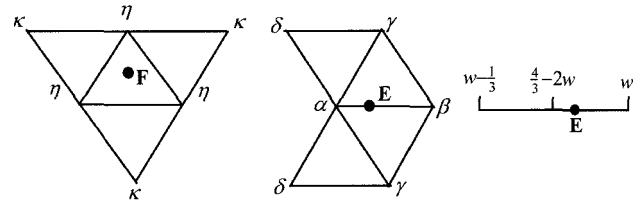

Fig. 10. The positions of some new points.

Fig. 11. The stencils of the ternary scheme with weight w.

where $\eta = \frac{2}{3} - w$, $\kappa = w - \frac{1}{3}$. The stencil of the new face-point is depicted in Fig. 11(left).

(2) One of the new edge-points E (see Fig. 10) for an interior edge are computed by

$$E = \alpha P_1 + \beta P_2 + \gamma(P_3 + P_4) + \delta(P_5 + P_6),$$

where $\alpha = \frac{4}{3} - 2w$, $\beta = -\frac{1}{3} + 2w$, $\gamma = \frac{1}{3} - w$, $\delta = -\frac{1}{3} + w$. The

stencil is depicted in Fig. 11(middle). The stencil of the other new edge-point is similar to this one.

(3) New edge-points for boundary edge are computed by (1). The corresponding stencil of a new edge-point is shown in Fig. 11(right). Similar to this we can get a result about the stencil of the other new boundary edge-point.

Remark: For triangles or edges, where some stencil points for the new face-point or the new edge-point may not exist, for example, the triangles near the boundary of the mesh, similar to [14] virtual points are introduced by reflecting vertices across the boundary of the mesh. With the help of the virtual points the normal new face-point and new edge-point rules can be used.

Similar to the method of eigenanalysis in [5] we know that the corresponding eigenvalues of the subdivision matrix are:

$$1, \frac{1}{3}, \frac{1}{3}, -\frac{5}{3} + 6w, -\frac{1}{3} + 2w(three\ times),$$

$$-\frac{1}{3} + w(six\ times), 0(six\ times),$$

which indicates that the limit surface could be C^1 only

for the range $\frac{2}{9} < w < \frac{1}{3}$. This is, unsurprisingly, the same

range of values of w as in the univariate and uniform case. But the actual continuity of the limit surface need a further analysis.

We can extend the above scheme to the case of non-uniform subdivision. But still the continuity of the limit surface is not known. Alternatively we may use the conversion method proposed in [15] and then apply the tensor-product 3-point ternary interpolatory subdivision scheme to the newly generated regular quadrilateral mesh. Based on the property of the tensor-product surface the continuity of the limit surface is easily gotten.

Except for the application in curve and surface modeling, the presented subdivision scheme may have

some potential application in some other areas, such as curve and surface metamorphosis, polygon morphing and so on, due to its local, ternary and controllable properties.

9. Conclusion

In this paper we have shown that in univariate non-uniform interpolating subdivision we can achieve the same smoothness with less number of control points by using a ternary rather than a binary subdivision scheme. So the subdivision schemes proposed in this paper have better locality. They can be used to model C^1 or C^0 interpolatory curves or surfaces whose shapes are controllable wholly or locally. Hence the presented algorithms are effective. Future work should aim at the continuity analysis on the scheme based on triangular mesh and the generalization of the presented schemes to the case of non-linear subdivision and general control nets.

Acknowledgements

References

[1] Cai, Z. J. (1995), Convergence, error estimation and some properties for four-point interpolation subdivision scheme, Computer Aided Geometric Design, 12(5), 459-468.

[2] Cai, Z. J. (1995), The theory and application of four-point scheme with non-stationary parameter, Chinese Annals of Mathematics (Ser. A), 16(4), 524-531 (in Chinese).

[3] Cai, Z. J. (1998) Modified four-point scheme and its application, Computer Aided Geometric Design, 15(2), 251-260.

[4] Deslauriers, G. and Dubuc, S., (1989), Symmetric iterative interpolation processes, Constructive Approximation, 5, 49-68.

[5] Dodgson, N.A., Sabin, M.A., Barthe, L., and Hassan,

M.F. (2002), Towards a ternary interpolating subdivision scheme for the triangular mesh, Technical Report number 539, University of Cambridge Computer Laboratory.

[6] Dyn, N., Gregory, J.A., and Levin, D. (1990), A butterfly subdivision scheme for surface interpolation with tension control, ACM Transactions on Graphics, 9, 160-169.

[7] Dyn, N., Levin, D., and Gregory, J.A. (1987), A 4-point interpolatory subdivision scheme for curve design, Computer Aided Geometric Design, 4(4), 257-268.

[8] Hassan, M.F. and Dodgson, N.A. (2002), Ternary and three-point univariate subdivision schemes, Curve and Surface Fitting: Saint-Malo 2002 (Albert Cohen, Jean-Louis Merrien, and Larry L. Schumaker eds.), pp.199-208.

[9] Hassan, M.F., and Dodgson, N.A. (2004), Further analysis of ternary and three-point univariate subdivision schemes, Technical Report number 599, University of Cambridge Computer Laboratory.

[10] Hassan, M.F., Ivrissimitzis, I.P., Dodgson, N.A., and Sabin, M.A. (2002), An interpolating 4-point C2 ternary stationary subdivision scheme, Computer Aided Geometric Design, 19(1), 1-18.

[11] Jin, J.R., and Wang, G.Z. (2000), A non-uniform 4-piont interpolatory subdivision scheme to construct curve, Appl. Math. J. Chinese Univ.(Ser. A), 15(1), 97-100 (in Chinese).

[12] Kobbelt, L. (1996), Interpolatory subdivision on open quadrilateral nets with arbitrary topology, Computer Graphics Forum (Proceedings of EUROGRAPHICS 1996), 15(3), 409-420.

[13] Kuijt, F. and Damme. R. (1998), Convexity-preserving interpolatory subdivision schemes, Constructive Approximation, 14(4), 609-630.

[14] Labisk, U. and Greiner, G. (2000), Interpolatory-subdivision, Compute Graphics Forum (Proceedings of EUROGRAPHICS 2000), 19(3), 131-138.

[15] Takayuki, Itoh. and Kenji, Shimada. (2002), Automatic conversion of triangular meshes into quadrilateral meshes with directionality, International Journal of CAD/CAM, 1(1), 11-21.

[16] Weissman, A. (1990), A 6-point interpolatory subdivision scheme for curve design, Master's thesis, Tel-Aviv University.

[17] Zorin, D., Schroder, P., and Sweldens, W. (1996), Interpolating subdivision for meshes with arbitrary topology, In Computer Graphics Proceedings, ACM SIGGRATH, 189-192.

Hongchan Zheng is a lecturer and a PhD student in the department of Applied Mathematics at Northwestern Polytechnical University, Xi'an, P.R. China. Her research interests include computer graphics and computer aided geometric design.

Zhenglin Ye is a professor in the department of Applied Mathematics at Northwestern Polytechnical University, Xi'an, P.R. China. His research interests include computer graphics, computer aided geometric design, fractal geometry and image processing.

Zuoping Chen is a PhD student in the department of Applied Mathematics at Northwestern Polytechnical University, Xi'an, P.R. China. His research interests include computer graphics and image processing.

Hongxing Zhao is a professor at Yulin College Shaanxi, Yulin P.R. China. His research interests include computer graphics, computer aided geometric design and image processing.
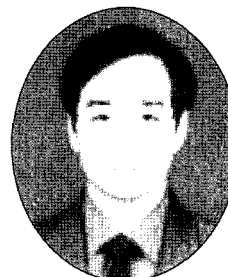
Hongchan Zheng   Zhenglin Ye   Zuoping Chen   Hongxing Zhao